International Journal of Computer Assisted Radiology and Surgery (2022) 17:619–625
https://doi.org/10.1007/s11548-022-02560-z

ORIGINAL ARTICLE

Prediction of pathological complete response using radiomics on MRI in patients with breast cancer undergoing neoadjuvant pharmacotherapy

Yuka Kuramoto[1] · Natsumi Wada[1] · Yoshikazu Uchiyama[2]

Received: 29 April 2021 / Accepted: 3 January 2022 / Published online: 12 January 2022

Abstract

Purpose Neoadjuvant pharmacotherapy is essential for patients with breast cancer who wish to preserve the breast by shrinking the malignant tumor, allowing breast-conserving surgery. It may eliminate cancer cells completely, which is known as pathologic complete response (pCR). Patients with pCR have a lower risk of recurrence. The purpose of this study was to develop a method for predicting patients who achieve pCR by neoadjuvant pharmacotherapy using radiomic features in MR images.

Methods Fat-suppressed T2-weighted MR images of 64 cases were identified from the ISPY1 dataset. There were 26 cases of pCR and 38 cases of non-pCR. The image slice with the largest tumor diameter was selected from MR images, and the tumor region was manually segmented. A total of 371 radiomic features were calculated from the tumor region. We selected nine radiomic features using Lasso in this study. A support vector machine (SVM) with nine radiomic features was used for predicting patients with pCR.

Results The result of the ROC analysis showed that the area under the curve of SVM was 0.92 for distinguishing between pCR and non-pCR. Although the input data contain data that were misclassified by SVM, the survival curve classified into the pCR group was at a higher position than the non-pCR group. However, the log-rank test was $p = 0.2$.

Conclusions We developed a method to predict patients with pCR by neoadjuvant pharmacotherapy using noninvasive MR images. The survival curve of patients classified as having pCR by the proposed method was higher than those classified as non-pCR. Since the proposed method predicts patients who achieve pCR by neoadjuvant pharmacotherapy, it enhances the value of preoperative image information.

Keywords Radiomics · Breast cancer · Neoadjuvant pharmacotherapy · Pathological complete response

Introduction

Mammography is a recognized screening method that has been effective in reducing breast cancer mortality. In Europe and America, the mortality rate is decreasing despite the increasing incidence of breast cancer because of high mammography screening rate. Since accurate detection of lesions is important in breast cancer screening, computer-aided diagnosis (CAD) [1–3] was developed to assist radiologists in the detection of breast cancer. Further, this has been the focus of artificial intelligence (AI) research for breast cancer.

On breast cancer diagnosis, it is important to remove the breast tumor by surgery. However, complete removal of the breast is being avoided to maintain quality of life after treatment. One of the factors is the recent advances in post-genomic research that increased the understanding of molecular biology of breast cancer, leading to the development of new drugs. The current standard of treatment for breast cancer is a multidisciplinary therapy that includes a medical approach using systemic therapy. In this type of treatment, the AI research that supports personalized treatment according to the biological characteristics of cancer is called Radiomics [4–20]. Medical care is performed in the order

✉ Yoshikazu Uchiyama
y_uchi@kumamoto-u.ac.jp

[1] Graduate School of Health Sciences, Kumamoto University, 4-24-1 Kuhonji, Chuo-ku, Kumamoto, Kumamoto 862-0976, Japan

[2] Department of Medical Image Sciences, Faculty of Life Sciences, Kumamoto University, 4-24-1 Kuhonji, Chuo-ku, Kumamoto, Kumamoto 862-0976, Japan

of disease detection, differential diagnosis, and treatment. Therefore, CAD can be considered an AI system supporting the first half of medical care, and radiomics is an AI system supporting the second half of medical care.

Breast cancer is characterized by the possibility of undetected metastasis. Therefore, drug systemic therapy is developed to be administered before and after surgery. The purpose of neoadjuvant pharmacotherapy is to (1) reduce the size of large tumor in patients who wish to preserve their breast, and (2) determine the sensitivity to drug therapy before surgery in patients who require adjuvant pharmacotherapy. Patients with pathological complete response (pCR) on neoadjuvant pharmacotherapy have a low risk of recurrence and have a better prognosis than patients without pCR [21, 22]. If achieving pCR can be predicted from the images, the value of preoperative image examination can be increased.

In predicting the effect of neoadjuvant pharmacotherapy, DEC-MRI (dynamic contrast-enhanced magnetic resonance imaging) [4–13], diffusion-weighted imaging [14–16], contrast-enhanced MRI [16, 17], and PET/CT [18–20] have been used. In this study, we developed a method for predicting pCR using fat-suppressed T2-weighted images that are commonly used in clinical practice. With regard to the biological characteristics of cancer, pCR patients with luminal B/HER2 (human epidermal receptor 2)-negative, HER2, and triple-negative tumors have a better prognosis than non-pCR patients. However, there was no significant difference between the prognosis of pCR and non-pCR in patients with luminal B/HER2-positive and luminal A breast cancers [21]. Since immunohistochemical staining can be used to classify the breast cancer subtypes, we can select patients who may have a better prognosis. However, the prognosis cannot be predicted. Therefore, in this study, we developed a method to predict pCR in patients with luminal B/HER2-negative, HER2, and triple-negative breast cancer. In addition, we applied the analysis of survival time using the prediction results of pCR and non-pCR to investigate whether there was a significant difference in the prognosis of the pCR group. This allows us to integrate the result of biopsy and imaging examination.

Materials and methods

Image database

We used a public database ISPY1 (investigation of serial studies to predict the therapeutic response with imaging and molecular analysis breast cancer) in TCIA (the cancer imaging archive) [23]. The ISPY1 contains MR images and clinical information of 221 patients with breast cancer. Fat-suppressed T2-weighted images were selected from 64 patients with luminal B/HER2 negative, HER2, and triple-negative tumors because of the significant difference in prognosis when these patients achieve pCR [21]. In this study, the immunohistochemically defined subtypes of breast cancer were determined, as shown in Table 1, using the information of PgR (progesterone receptor), ER (estrogen receptor), and HER2. There were 26 cases of pCR (4 cases of luminal B/HER2-negative, 7 cases of HER2, and 15 cases of triple-negative) and 37 cases of non-pCR (10 cases of luminalB/HER2-negative, 10 cases of HER2, and 18 cases of triple-negative). Information on hormone receptor, HER2, pCR, and survival time was attached to the database. All MR images were converted to 512×512 by linear interpolation. The patients' ages ranged from 26 to 68 years. The tumor diameters ranged from 2.1 to 13.7 cm and median of 5.2 cm. The mean and standard deviation of tumor diameter for pCR and non-pCR cases were 5.4 ± 3.1 cm and 6.1 ± 2.5 cm, respectively. The result of t test was $p = 0.3$, which was not significantly different. This study was approved by the ethical review committee.

Table 1 The immunohistochemistry defined subtypes of breast cancer

	Hormone receptor		HER2
	ER	PgR	
Luminal A	+	+	−
Luminal B (HER2 negative)	+	−	
	−	+	
Triple-negative breast cancer (TNBC)	−	−	
Luminal B (HER2 positive)	+	+	+
		−	
HER2 type	−	−	

Tumor segmentation

The image slice with the largest tumor diameter was selected from the MR images, and the tumor region was manually segmented. According to the rules of marking, when there are multiple tumors in the MR image, the largest tumor area should be selected. We marked the spicules and incorrect edges as the tumor region to accurately quantify the radiomic features related to the shape. Radiological technologist certified in mammography segmented all tumor regions by using a free software MaZda [24–26]. Radiologists checked the segmented regions, and made corrections if necessary. Figure 1 shows an example of marking the tumor region.

Radiomic features

To normalize the pixel values, we performed a linear density transformation on all MR images. When the linear density

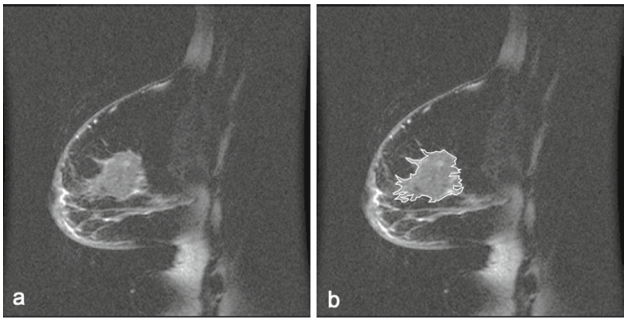

Fig. 1 Example of a manually segmented tumor region. **a** Original image and **b** segmented tumor region

transformation was applied, the maximum pixel value was affected by noise due to high pixel values. The width of the pixel value became small in the tumor region. To solve this problem, we calculated the upper 0.01%-pixel value of the density histogram and set the pixel values above the pixel value as 1023. The linear density transformation was performed so that the minimum and maximum pixel values were 0 and 1023, respectively. We assumed that the noise existed in 0.01% of the entire image and determined the value empirically.

We calculated 371 radiomic features from the tumor region of the MR image after linear density transformation. The MaZda was used to calculate the radiomic features. The 371 radiomic features included 74 shape, 9 histogram, 272 texture, and 16 resolution. The default values of MaZda were used as parameters for calculating these 371 radiomic features. For example, the parameters when calculating the density co-occurrence matrix of texture features were 16 density gradations, 1–5 in the distance between pixels, and 0°, 45°, 90°, and 135° in the direction.

Selection of radiomic features

There were 371 radiomic features and 64 cases hence, it is necessary to select useful radiomic features for the prediction of pCR. In this study, the radiomic features were selected using the least absolute shrinkage and selection operator (Lasso) [27], which is determined by the following equation:

$$\hat{\beta}^{\text{lasso}} = \arg\min_{\beta} \left\{ \frac{1}{2} \sum_{i=1}^{N} \left(y_i - \beta_0 - \sum_{j=1}^{p} x_{ij} \beta_j \right)^2 + \lambda \sum_{j=1}^{p} |\beta_j| \right\} \quad (1)$$

where y_i is the pCR or non-pCR of the ith patient. x_j are radiomic features. β_j are coefficients, and β_0 is a constant term. $\lambda \geq 0$ is a complexity parameter that controls the degree of reduction. p represents the total number of radiomic features. The parameter β_j can be obtained by solving the quadratic programming problem in Eq. (1). In this study, λ was set such that the number of radiomic features whose β_j was not zero but nine. A tenfold cross validation was performed to determine the value of λ that minimizes the average deviation. When the values of λ obtained in the process of this calculation were used in order, the value of λ was adopted so that the number of radiomic features with nonzero coefficient β_j was nine.

Prediction of pCR

The classifier with 9 radiomic features selected by Lasso was used to distinguish between pCR and non-pCR. As the classifier, we used linear discriminant analysis (LDA) [28] and a support vector machine (SVM) [29]. LDA is a method of finding a hyperplane when the variances of the pCR and non-pCR groups are the same in the feature space where the radiomic features are used as input variables. The problem of LDA is the discrimination boundary that is pulled in the direction of outliers which is different with other cases. In addition, when the pCR and non-pCR groups cannot be linearly separated in the feature space, high discrimination performance cannot be obtained. However, if high discrimination performance is obtained by LDA, it means that the pCR and non-pCR groups can be distinguished by a simple rule of feature space. Therefore, radiomic features may be used as an image biomarker for classifying pCR and non-pCR.

On the other hand, SVM can remove the outliers using a technique called soft margin and create a discrimination boundary. Thus, it is not affected by outliers. Moreover, a highly accurate discrimination is possible even without linear separation because a complicated discrimination boundary can be made by a kernel trick. By comparing the discriminant scores of LDA and SVM, we can understand how complex pCR and non-pCR groups overlap in the feature space. The leave-one-out method [30] was used for training and for testing the classifiers. The discrimination performance was evaluated by performing receiver operating characteristic (ROC) analysis using the LABROC4 algorithm [31] from the University of Chicago.

Survival time analysis

By applying the method described in the previous section, it is possible to distinguish between the pCR and non-pCR groups. The proposed method is proven useful for the prognostic prediction of neoadjuvant pharmacotherapy if there is a significant difference in the survival time of patients predicted to have pCR even if the discriminative ability of the proposed method is not high. Therefore, we performed a survival time analysis with the discrimination results between the pCR and non-pCR groups as input data. At this time,

we conducted the experiment by collecting the survival time of the 62 patients from the ISPY1 database. By using Kaplan–Meier [32], the two survival curves were obtained by estimating the cumulative hazard functions of the pCR and non-pCR groups discriminated by the proposed method. The log-rank test [32] was performed on the two survival curves to calculate if there is a statistically significant difference.

Results

Figure 2 shows the relationship between the number of radiomic features selected by Lasso and the LDA discrimination results. The number of radiomic features depends on the value of the Lasso reduction parameter λ. The discrimination performance of LDA was obtained when the number of radiomic features was increased from 2 to 10 by changing the value of λ. The result showed that the discrimination performance was highest when 9 radiomic features were used. Table 2 shows the nine selected radiomic features. Four shape features, 4 texture features, and 1 resolution feature were selected. Figure 3 shows the ROC curves of LDA and SVM when these 9 radiomic features were used as input data. A Gaussian kernel was used for the SVM. The area under the curve (AUC) of LDA and SVM were 0.75 and 0.92, respectively. The discrimination performance of SVM was higher than LDA. This means that pCR and non-pCR groups are not distributed in a simple relationship that can be distinguished by a hyperplane in the 9 radiomic feature space. Table 3 shows the discrimination results using SVM.

The sensitivity was 92.3%, and the specificity was 71.1% for distinguishing between pCR and non-pCR. Figure 4a shows the result of the survival time analysis when this discrimination result of SVM was used as input data. It should be noted that the input data contain data that were misclassified by SVM. The survival curve classified into the pCR group

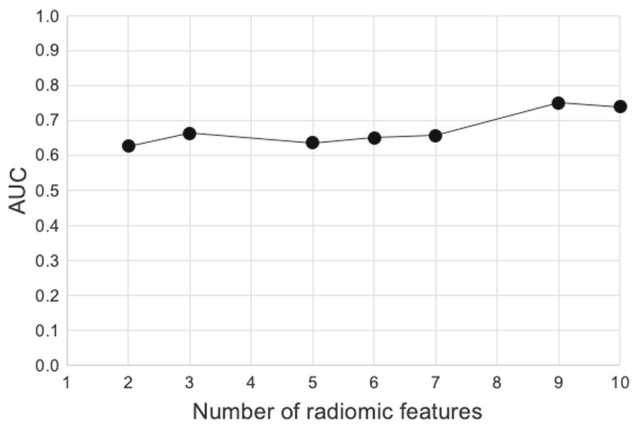

Fig. 2 Relationship between the number of radiomic features and the classification performance of LDA

Table 2 Nine radiomic features selected by Lasso

	Radiomic feature	Category	Description
#1	GeoAox	Geometry	Oriental angle
#2	GeoW9	Geometry	Area of the circumscribing rectangle/number of the object pixels
#3	GeoW13	Geometry	Maximal diameter/number of the object pixels
#4	GeoYo	Geometry	Gravity center to inscribed circle center distance
#5	S(1,1) Contrast	Texture	Contrast of co-occurrence matrix (S(1,1) is the between-pixels distance)
#6	Vertl_GLevNonU	Texture	Vertical grey level nonuniformity of run length matrix
#7	GrKurtosis	Texture	Absolute gradient kurtosis
#8	Teta1	Texture	Parameter θ_1 in the autoregressive model
#9	WavEnHH_s-1	Resolution	Wavelet energy (frequency band: HH, scale: 1rd)

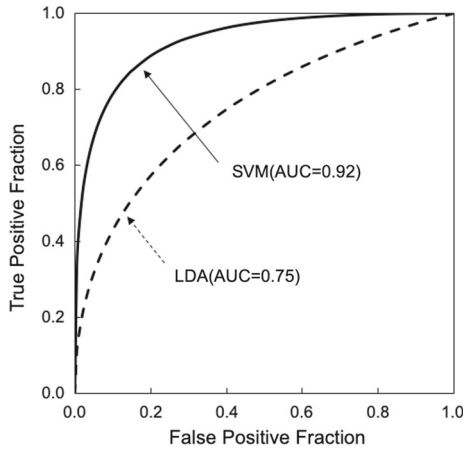

Fig. 3 ROC curves for distinguishing between pCR and non-pCR

was at a higher position than the non-pCR group. However, the log-rank test was $p = 0.2$ and there was no significant difference found. Figure 4b shows the survival curves when all of them were correctly classified. The survival curve of the pCR group was higher than the non-pCR group, and the log-rank test was $p = 0.003$. Therefore, if the discriminative performance of the proposed method can be further improved by using deep learning, it can be claimed that the prognosis of patients predicted to have pCR is good.

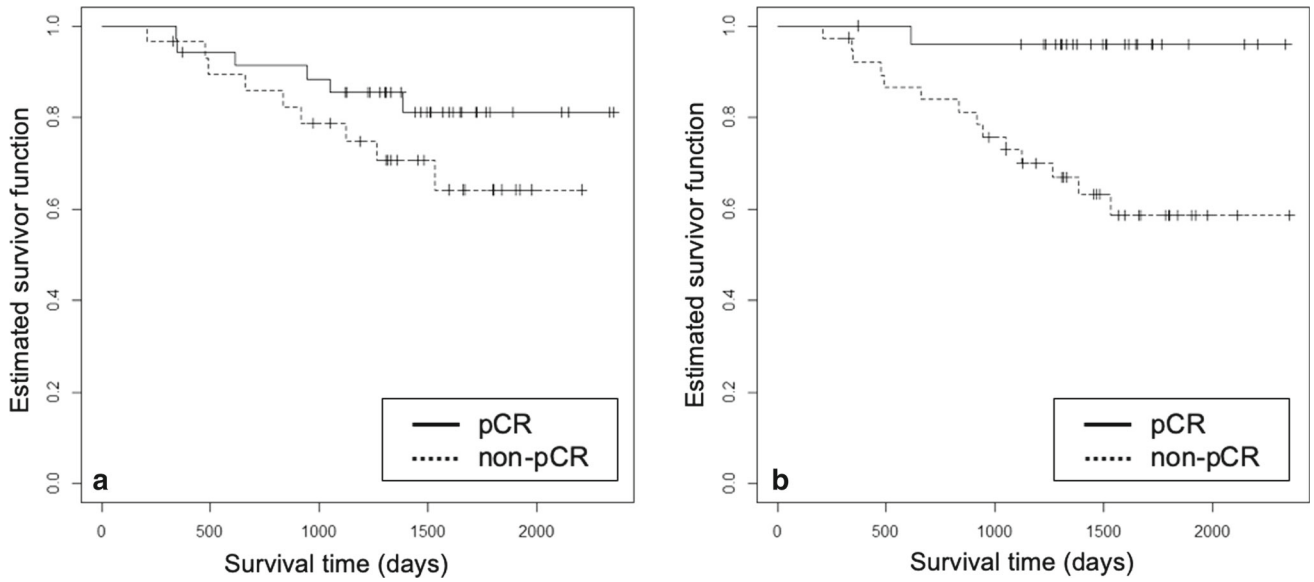

Fig. 4 Kaplan–Meier estimate of survivor functions. **a** When we use the prediction results of SVM. **b** When we use the truth data, which accurately classify all cases

Table 3 Classification performance of SVM

	Computer output	
	pCR	Non-pCR
Truth		
pCR	92.3% (24/26)	7.7% (2/26)
Non-pCR	28.9% (11/38)	71.1% (27/38)

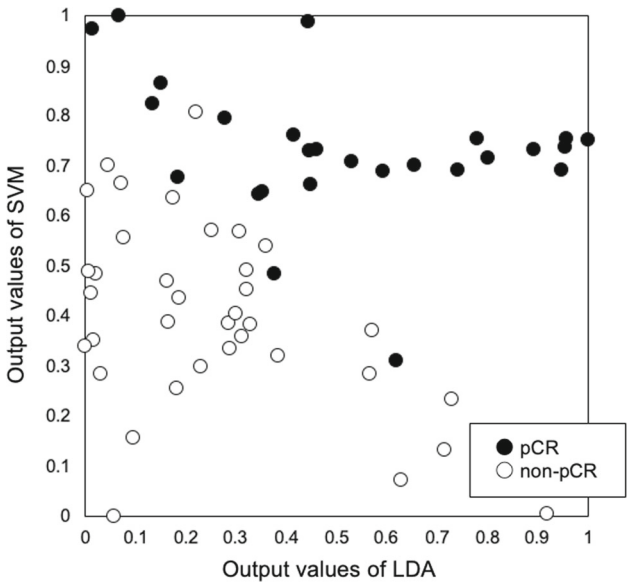

Fig. 5 Relations of output values between LDA and SVM

Discussion

When the proposed method is used in the clinical practice, radiologists can use the radiomic feature as an imaging biomarker in their image interpretation if there is a simple relationship between radiomic features and prediction of pCR. For example, if lesion having complicated shape or large size can be easily assumed as pCR, shape or size can be used as imaging biomarker. Hence, it is important to find out whether there is such a simple relationship or not. In Fig. 5, the horizontal axis shows the output values of LDA and the vertical axis shows the output values of SVM. When the LDA on the horizontal axis is used, it is difficult to distinguish the pCR group from the non-pCR group; however, when SVM on the vertical axis is used, the degree of separation between the pCR and non-pCR groups is improved. LDA is a method for determining a hyperplane in a multidimensional space, and SVM is a method of forming a more complex decision surface than LDA. Therefore, this result indicates that the relationship between radiomics features measured from fat-suppressed T2-weighted images and the pCR or non-pCR group is quite complicated. Thus, radiologists cannot use radiomic features as imaging biomarkers.

We investigated related researches to investigate the existence of imaging biomarker for prognostic prediction or molecular diagnosis when we used other images. Cain et al. conducted an experiment on triple-negative and HER2 positive breast cancer [8]. They reported that the AUC value of logistic regression using four radiomic features measured from DCE-MRI was 0.707. Liu et al. selected four radiomic features from the T2-weighted image, diffusion-weighted image, and contrast-enhanced T1-weighted image by using

the Boruta algorithm [16]. By using SVM, the AUC value for discriminating between pCR and non-pCR groups was 0.79. These results also indicate that it is difficult to find imaging biomarkers associated with the pCR group. On the other hand, from a patient's perspective, it is sufficient to select the optimal treatment for cancer, and radiomic features used in AI may act as a black box. We recommend further studies to investigate its use in the clinical practice.

Similar studies have been conducted for the discrimination of benign and malignant CAD [1, 2]. CAD is a study for discriminating the current state x_t from the current image, but this study predicts the future state x_{t+1} from the current image. CAD for discriminating benign and malignant conditions has a drawback; if a malignant cancer is misclassified as benign, the patient may lose the opportunity for treatment. For this reason, various functions such as presenting the quantified value of image features and similar cases of benign or malignant have been developed [33] in order to improve the radiologist's diagnostic accuracy with CAD. Thus, considerable time was required for its practical application. However, the present study included malignant cancers, and surgery is performed even if our system mistakenly predicts that neoadjuvant pharmacotherapy will not be effective. Therefore, even if our system makes an erroneous decision, it does not strongly result in a bad decision, and may not be a major problem in actual operation. Therefore, radiomics AI system is considered easier to put into practical use than CAD for the differential diagnosis. However, it should be noted that there is a possibility of unnecessary pharmacotherapy.

The limitation of present study is the number of cases is small because of using the selected subtypes of breast cancer. It is necessary to confirm the usefulness of the proposed method using a large database.

Conclusion

We developed a method to predict patients with pCR by neoadjuvant pharmacotherapy using noninvasive MR images. The survival curve of patients classified as having pCR by the proposed method was higher than those classified as non-pCR. By improving the discrimination performance of our method, the prognosis of patients predicted to have pCR was good. The proposed system can enhance the value of preoperative image examination.

Acknowledgements A part of this study was supported by a Grant-in-Aided for Scientific Research (C) (No.21K12707) and a grant from Suzuken Memorial Foundation.

References

1. Doi K (2007) Computer-aided diagnosis in medical imaging: historical review, current status and future potential. Comput Med Imaging Graph 31:198–211
2. Giger ML (2004) Computerized analysis of images in the detection and diagnosis of breast cancer. Semin Ultrasound CT MR 25:411–418
3. Li Q, Nishikawa RM (2015) Computer-aided detection and diagnosis in medical imaging. CRC Press, Florida
4. Ma W, Zhao Y, Ji Y, Guo X, Jian X, Liu P, Wu S (2019) Breast cancer molecular subtype prediction by mammographic radiomic features. Acad Radiol 26(2):196–201
5. Li H, Zhu Y, Burnside ES, Huang E, Drukker K, Hoadley KA, Fan C, Conzen SD, Zuley M, Net JM, Sutton E, Whitman GJ, Morris E, Perou CM, Ji Y, Giger ML (2016) Quantitative MRI radiomics in the prediction of molecular classifications of breast cancer subtypes in the TCGA/TCIA data set. NPJ Breast Cancer 2:16012
6. Wang J, Kato F, Oyama-Manabe N, Li R, Cui Y, Tha KK, Yamashita H, Kudo K, Shirato H (2015) Identifying triple-negative breast cancer using background parenchymal enhancement heterogeneity on dynamic contrast-enhanced MRI: a pilot radiomics study. PLoS ONE 10(11):e0143308
7. Cao K, Zhao B, Li XT, Li YL, Sun YS (2019) Texture analysis of dynamic contrast-enhanced MRI in evaluating pathologic complete response (pCR) of mass-like breast cancer after neoadjuvant therapy. J Oncol 4731532
8. Cain EH, Saha A, Harowicz MR, Marks JR, Marcom PK, Mazurowski MA (2019) Multivariate machine learning models for prediction of pathologic response to neoadjuvant therapy in breast cancer using MRI features: a study using an independent validation set. Breast Cancer Res Treat 173:455–463
9. Heacock L, Lewin A, Ayoola A, Moccaldi M, Babb JS, Kim SG, Moy L (2020) Dynamic contrast-enhanced MRI evaluation of pathologic complete response in human epidermal growth factor receptor 2 (HER2)-positive breast cancer after HER2-targeted therapy. Acad Radiol 27:e87–e93
10. Drukker K, Edwards A, Doyle C, Papaioannou J, Kulkarni K, Giger ML (2019) Breast MRI radiomics for the pretreatment prediction of response to neoadjuvant chemotherapy in node-positive breast cancer patients. J Med Imaging 6:034502
11. Fusco R, Granata V, Maio F, Sansone M, Petrillo A (2020) Textural radiomic features and time-intensity curve data analysis by dynamic contrast-enhanced MRI for early prediction of breast cancer therapy response: preliminary data. Eur Radiol Exp 4(1):8
12. Braman NM, Etesami M, Prasanna P, Dubchuk C, Gilmore H, Tiwari P, Plecha D, Madabhushi A (2017) Intratumoral and peritumoral radiomics for the pretreatment prediction of pathological complete response to neoadjuvant chemotherapy based on breast DCE-MRI. Breast Cancer Res 19(1):57
13. Braman N, Prasanna P, Whitney J, Singh S, Beig N, Etesami M, Bates DDB, Gallagher K, Bloch BN, Vulchi M, Turk P, Bera KM, Abraham J, Sikov WM, Somlo G, Harris LN, Gilmore H, Plecha D, Varadan V, Madabhushi A (2019) Association of peritumoral radiomics with tumor biology and pathologic response to preoperative targeted therapy for HER2(ERBB2)-positive breast cancer. JAMA Netw Open 2(4):e192561
14. Santamaría G, Bargalló X, Fernández PL, Farrus B, Caparros X, Velasco M (2017) Neoadjuvant systemic therapy in breast cancer: association of contrast-enhanced MR imaging findings, diffusion-weighted imaging findings, and tumor subtype with tumor response. Radiology 283(3):663–672
15. Chen X, Chen X, Yang J, Li Y, Fan W, Yang Z (2020) Combining dynamic contrast-enhanced magnetic resonance imaging and apparent diffusion coefficient maps for a radiomics nomogram to

predict pathological complete response to neoadjuvant chemotherapy in breast cancer patients. J Comput Assist Tomogr 44:275–283
16. Liu Z, Li Z, Qu J, Zhang R, Zhou X, Li L, Sun K, Tang Z, Jiang H, Li H, Xiong Q, Ding Y, Zhao X, Wang K, Liu Z, Tian J (2019) Radiomics of multiparametric MRI for pretreatment prediction of pathologic complete response to neoadjuvant chemotherapy in breast cancer: a multicenter study. Clin Cancer Res 25(12):3538–3547
17. Zhou J, Lu J, Gao C, Zeng J, Zhou C, Lai X, Cai W, Xu M (2020) Predicting the response to neoadjuvant chemotherapy for breast cancer: wavelet transforming radiomics in MRI. BMC Cancer 20(1):100
18. Li P, Wang X, Xu C, Liu C, Zheng C, Fulham MJ, Geng D, Wang L, Song S, Huang G (2020) 18F-FDG PET/CT radiomic predictors of pathologic complete response (pCR) to neoadjuvant chemotherapy in breast cancer patients. Eur J Nucl Med Mol Imaging 47(5):1116–1126
19. Antunovic L, De Sanctis R, Cozzi L, Kirienko M, Sagona A, Torrisi R, Tinterri C, Santoro A, Chiti A, Zelic R, Solloni M (2019) PET/CT radiomics in breast cancer: promising tool for prediction of pathological response to neoadjuvant chemotherapy. Eur J Nucl Med Mol Imaging 46(7):1468–1477
20. Ha S, Park S, Bang JI, Kim EK, Lee HY (2017) Metabolic radiomics for pretreatment 18F-FDG PET/CT to characterize locally advanced breast cancer: histopathologic characteristics, response to neoadjuvant chemotherapy, and prognosis. Sci Rep 7(1):1556
21. Minckwitz GV, Untch M, Blohmer JU, Cosa SD, Eidtmann H, Fasching PA, Gerber B, Eiermann W, Hilfrich J, Huober J, Jackisch C, Kaufmann M, Konecny GE, Denkert C, Nekljudova V, Mehta K, Loibl S (2012) Definition and impact of pathologic complete response on prognosis after neoadjuvant chemotherapy in various intrinsic breast cancer subtypes. J Clin Oncol 30(15):1796–1804
22. Broglio KR, Quintana M, Foster M, Olinger M, McGlothlin A, Berry SM, Boileau JF, Brezden-Masley C, Chia S, Dent Sm Gelmon K, Paterson A, Rayson D, Berry DA (2016) Association of pathologic complete response to neoadjuvant therapy in HER2-positive breast cancer with long-term outcomes: a meta-analysis. JAMA Oncol 2(6):751–760
23. TCIA. https://wiki.cancerimagingarchive.net/display/Public/ISPY1. Accessed 29 April 2021
24. Technical University of Lodz. http://eletel.eu/mazda. Accessed 29 April 2021
25. Szczypiński PM, Strzelecki M, Materka A, Klepaczko A (2009) MaZda–a software package for image texture analysis. Comput Methods Programs Biomed 94(1):66–76
26. Strzelecki M, Szczypinski P, Materka A, Klepaczko A (2013) A software tool for automatic classification and segmentation of 2D/3D medical images. Nucl Instrum Methods Phys Res 702:137–140
27. Hastie T, Tibshirani R, Friedman J (2009) The elements of statistical learning, data mining, inference and prediction, 2nd edn. Springer, New York
28. Duda RO, Hart PE, Stork DG (2001) Pattern classification. Wiley, New York
29. Abe S (2005) Support vector machines for pattern classification. Springer, London
30. Theodoridis S, Koutroumbas K (1999) Pattern recognition. Academic Press, London
31. Metz CE (1989) Some practical issues of experimental design and data analysis in radiological ROC studies. Investig Radiol 24:234–245
32. Collett D (2003) Modelling survival data in medical research, 2nd edn. Chapman & Hall CRC, Boca Raton
33. Muramatsu C (2018) Overview on subjective similarity of images for content-based medical image retrieval. Radiol Phys Technol 11:109–124